

DOI: 10.1002/cphc.200900822

Protein Conformational Dynamics of Homodimeric Hemoglobin Revealed by Combined Time-Resolved Spectroscopic Probes

Jungkweon Choi,^[a] Srinivasan Muniyappan,^[a] John T. Wallis,^[a] William E. Royer, Jr.,^[b] and Hyotcherl Ihee*^[a]

Allostery is an important mechanism to control protein activity through a series of discrete conformational changes that alter the oligomeric protein structure and ligand affinity. In this regard, the homodimeric hemoglobin (Hbl, see Figure 1) from

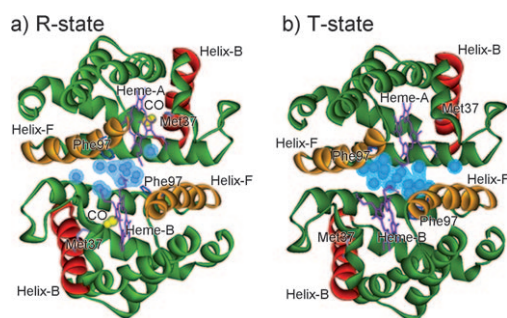


Figure 1. Crystal structure of a) R-state (PDB code: 3SDH) and b) T-State (PDB code: 4SDH) showing the heme (stick model-violet), subunit interface water molecules (wire mesh model-sky blue) and two CO molecules (space filled model-yellow). The helices B and F are highlighted in red and orange respectively and the key residues Phe97 (Blue) and Met37 (Bluish grey) are represented by a stick model.

the invertebrate *Scapharca inaequivalvis* is the simplest protein to study allostery and cooperative ligand binding because of its homodimeric structure when compared with the tetrameric mammalian hemoglobin (Hb), a standard paradigm for studying the allosteric regulation.^[1] Here we report that a combination of time-resolved spectroscopic probes is necessary to provide convincing and comprehensive assignments of protein kinetics. Our comparative results using both transient absorption spectroscopy and transient grating techniques show that transient absorption spectroscopy is sensitive to the protein relaxation that takes place in the heme environment of proteins, but can be blind to the overall quaternary structural change.

Hbl shows highly cooperative ligand binding with a Hill coefficient of 1.5 and mainly tertiary structural changes rather

than quaternary structural changes due to the ligand binding,^[2,3] whereas the cooperativity of Hb reveals large quaternary structural as well as tertiary structural changes.^[4–7] For instance, after the photodissociation of the ligand, allosteric changes in Hbl are tightly coupled with tertiary structural changes that include the heme–heme interaction due to the relocalization of the heme groups,^[8,9] the reorganization of interfacial water molecules at the subunit interface^[10] and the F helix phenylalanine flipping.^[9–11] For the quaternary structural changes, a small subunit rotation of 3.3° is estimated to occur based on the comparison of the static X-ray crystal structures of the liganded and unliganded Hbl.^[8,9] In time-resolved X-ray crystallographic studies,^[12] a Hbl mutant (M37 V) with lower geminate rebinding was used and thus the yield of the structural transition is higher than with the wild type. Although the mutant has an enlarged distal pocket, it maintains cooperative ligand binding and undergoes the same ligand-linked structural transitions as wild-type Hbl.

In this study, the conformational dynamics and thermodynamics of Hbl in solution phase have been investigated using time-resolved photothermal spectroscopic techniques such as the laser-induced transient grating (TG) and photoacoustic (PA) calorimetric techniques as well as the typical transient absorption (TA) spectroscopy. The TG technique is a powerful tool to monitor the spectrally silent dynamics such as changes in molecular energy, volume or interactions during chemical reactions.^[13–16] It had been accepted that the transition from R state (oxy-form) to T state (deoxy-form) of Hbl in solution phase takes place at a rate of 0.5–2 μs. In this study, however, we found ~1.4 μs kinetics, which is observed by both the TA and TG techniques, may be attributed to the absorption change of the heme group in Hbl rather than the full R–T transition of Hbl. Furthermore, the quantitative analysis of TG signals reveal a new dynamics of ~8.7 μs, which was not observed by the TA technique and may be attributed to the molecular volume change due to the R to T quaternary structural change. PA and TG measurements of the volume changes associated with these processes allow us to link the two processes to the entry of water molecules into the dimeric interface. In addition, from the measurement of the temperature-dependent TA and PA signals, we also determined the thermodynamic properties for the formation of the tertiary Hbl intermediate upon the photodissociation reaction of HbICO. Our results show that the combination of complementary probes allows a more convincing and comprehensive assignment of the observed timescales to tertiary and quaternary structural transitions and corrects some of previous kinetic assignments, underscoring the importance of employing combined probes.

[a] Dr. J. Choi,^{*} S. Muniyappan,^{*} Dr. J. T. Wallis, Prof. H. Ihee
Center for Time-Resolved Diffraction, Department of Chemistry
Graduate School of Nanoscience & Technology (WCU), KAIST
Daejeon 305-701 (Republic of Korea)
Fax: (+82) 42-869-2810
E-mail: hyotcherl.ihee@kaist.ac.kr

[b] P. W. E. Royer, Jr.
Department of Biochemistry and Molecular Pharmacology
University of Massachusetts, Medical School, Worcester MA 01655 (USA)

[*] These authors contributed equally to this work.

Supporting information for this article is available on the WWW under <http://dx.doi.org/10.1002/cphc.200900822>.

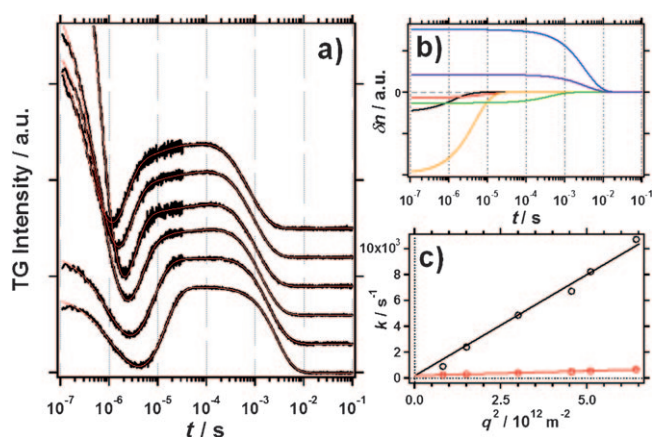


Figure 2. a) Time profiles of the transient grating signals after photoexcitation at 532 nm of HbICO in a 100 mM phosphate buffer (pH 7) at various q^2 ranges (from top to bottom, $q^2 = 6.42, 5.10, 4.55, 3.00, 1.50$ and $0.82 \times 10^{12} \text{ m}^{-2}$). The theoretical fits obtained from the global fitting analysis are shown in red. The observed TG signals are well reproduced by Equation (1). b) Decomposition of the components of the TG signal at $q^2 = 1.50 \times 10^{12} \text{ m}^{-2}$ according to Equation (1). c) Plots of the decay rate constants, k_{CO} (black circle) and k_{Hbl} (red circle), of the TG signals against q^2 . From the slope of the plot, the diffusion coefficients of CO and Hbl are determined to be $1.6 \pm 0.4 \times 10^{-9} \text{ m}^2 \text{ s}^{-1}$ and $0.74 \pm 0.03 \times 10^{-10} \text{ m}^2 \text{ s}^{-1}$, respectively. Furthermore, the intercept of the plot at $\tau = 5.3 \pm 0.4 \text{ ms}$ represents the CO ligand recombination rate.

Figure 2a shows TG signals of Hbl after photoexcitation of HbICO at various q^2 values. All TG signals for the Hbl samples rise quickly after photoexcitation within the instrumental response time of our system and then reveal a weak slowly rising component. The signals then show a decay component on a few-microseconds timescale, again rise within several ten microseconds and finally decay to the baseline with a lifetime of milliseconds. Considering the thermal diffusivity in the experimental condition, the dynamics observed in the few-microsecond timescale should include the contribution of the thermal grating produced by the thermal energy coming from the nonradiative transition and the enthalpy change of the reaction. An initial attempt to fit the TG signal with a simple equation revealed that the rate constants of two fast components show a constant value regardless of q^2 , meaning that these dynamics are the reaction kinetics followed after the photodissociation of the CO ligand, not those of the diffusion processes of chemical species involved in the photodissociation reaction of HbICO. From the q^2 dependent TG signals as depicted in Figure 2a, the slower dynamics (~submillisecond and millisecond) is attributed to the diffusion processes of species such as HbICO, Hbl and CO. Since the molecular sizes of Hbl and HbICO are very similar, the diffusion coefficients of two species are similar ($D_{\text{Hbl}} \approx D_{\text{HbICO}}$). The constant background between fast dynamics and slow dynamics reflects the δk_{Hbl} component, (see Supporting Information for details), which can be attributed to an absorption change of the band III of the protein (HbICO \rightarrow Hbl + CO). We fit all TG signals by minimizing the discrepancy between the experimental curves for all q^2 values (global fitting analysis) and theoretical curves represented by Equation (1) [see the Supporting Information for details]:

$$I_{\text{TG}} = \alpha \left[\begin{aligned} &\delta n_{\text{th}} \exp(-D_{\text{th}} q^2 t) + \delta n_{\text{f1}} \exp(-k_{\text{f1}} t) \\ &+ \delta n_{\text{f2}} \exp(-k_{\text{f2}} t) - \delta n_{\text{CO}} \exp(-k_{\text{CO}} t) + \delta n_{\text{Hbl}} \exp(-k_{\text{Hbl}} t) \end{aligned} \right]^2 + \beta [\delta n_{\text{Hbl}} \exp(-k_{\text{Hbl}} t)]^2 \quad (1)$$

where k_{f1} and k_{f2} are the rate constants of the two fast components.

The results of a global fitting analysis are depicted in Figure 2a. The observed TG signals are well reproduced by Equation (1). From the result of the global fitting analysis, two rate constants of the q^2 -independent components (k_{f1} and k_{f2}) are determined to be $7.4 \pm 2.0 \times 10^5 \text{ s}^{-1}$ ($1.4 \pm 0.4 \mu\text{s}$) and $1.2 \pm 0.6 \times 10^5 \text{ s}^{-1}$ ($8.7 \pm 4.3 \mu\text{s}$), respectively. The diffusion coefficients of CO and Hbl are determined from the plot of the decay rate constants, k_{CO} and k_{Hbl} , from the fitting of the species grating signal as a function of q^2 by using Equation (S6) in the Supporting Information. As shown in Figure 2c, both rate constants show a good linear relationship against q^2 . From the slope of the plot, the diffusion coefficients of CO and Hbl are calculated to be $1.6 (\pm 0.4) \times 10^{-9} \text{ m}^2 \text{ s}^{-1}$ and $0.74 (\pm 0.03) \times 10^{-10} \text{ m}^2 \text{ s}^{-1}$, respectively. Furthermore, the intercept of the plot at $\tau = 5.3 \pm 0.4 \text{ ms}$ represents the CO ligand recombination rate. The observed D_{CO} ($1.6 \times 10^{-9} \text{ m}^2 \text{ s}^{-1}$) is consistent with that of CO reported previously ($1.46 \sim 3.1 \times 10^{-9} \text{ m}^2 \text{ s}^{-1}$).^[15,17] On the other hand, the D_{Hbl} ($0.73 \times 10^{-10} \text{ m}^2 \text{ s}^{-1}$), determined from the TG method, is compared with that calculated from the molecular weight of Hbl ($M_{\text{Hbl}}: \sim 32.1 \text{ kDa}$). Young et al. reported that the size and volume of a protein can be determined from its molecular weight because the partial specific volume of a protein has a mean value of $0.73 \text{ cm}^3 \text{ g}^{-1}$, and they proposed the empirical Equation (2) to calculate the diffusion coefficient of a protein.^[18]

$$D = 8.34 \times 10^{-8} \frac{T}{(\eta M^{1/3})} \quad (2)$$

where T is temperature, η is the solvent viscosity and M is the molecular weight of a protein. From Equation (2), the diffusion coefficient of Hbl is calculated to be $\sim 0.75 \times 10^{-10} \text{ m}^2 \text{ s}^{-1}$. This value is consistent with that of the Hbl determined from TG signals ($0.74 \times 10^{-10} \text{ m}^2 \text{ s}^{-1}$).

Here, we consider the origins of two rate constants (k_{f1} and k_{f2}) observed in the few-microsecond time region. Candidate processes responsible for these ($1.4 \mu\text{s}$ and $8.7 \mu\text{s}$) are as follows: 1) the geminate recombination of the CO ligand, 2) the tertiary structural changes such as the relaxation of the heme propionate groups toward their T-state and packing of the F4 Phe in contact with the heme, or 3) the quaternary subunit rotation from R state to T state. It has been widely accepted that the R-T transition of Hbl in solution takes place with a rate of $0.5 \sim 2 \mu\text{s}$ based on the TA signals.^[19,20] Chiancone and co-workers reported^[19] that after the photoexcitation, 5% of the dissociated CO ligand geminately rebinds to iron with the rate constant of $1.4 \times 10^7 \text{ s}^{-1}$ (71 ns), and there is an absorbance change of deoxyHbl following photolysis at a rate constant of $1.2 \times 10^6 \text{ s}^{-1}$ (0.83 μs). Nichols and co-workers reported^[20] that

the absorbance change associated with the allosteric transition between R and T states occurs with a rate constant of $2 \times 10^6 \text{ s}^{-1} \sim 5 \times 10^5 \text{ s}^{-1}$ (0.5–2.0 μs). Rousseau and co-workers reported^[21] that the transient form relaxes to the deoxy structure concertedly with a half-life of 1 μs , and attributed this time-scale to tertiary relaxations. In order to further examine the conformational dynamics of Hbl following after the photodissociation of CO ligand, we conducted our own TA experiment in a 100 mM phosphate buffer solution (pH 7) at 298 K and the result is depicted in Figure 3.

Table 1. Decay times (τ) with pre-exponential factors (a) for Hbl from TA signals measured at various temperatures at monitoring wavelength 435 nm.

Temp. [K]	a_1	τ_1 [ns]	$a_2 (\pm 0.01)$	τ_2 [μs]	$a_3 (\pm 0.01)$	τ_3 [ms]
275	0.04 ± 0.01	387 ± 122	-0.06	9.80 ± 0.67	0.49	11.8 ± 0.1
283	0.06 ± 0.02	208 ± 72	-0.08	7.90 ± 0.41	0.56	7.5 ± 0.1
288	0.07 ± 0.09	101 ± 87	-0.08	4.14 ± 0.24	0.57	5.7 ± 0.1
293	-	-	-0.08	3.11 ± 0.16	0.59	4.4 ± 0.1
295	-	-	-0.09	2.31 ± 0.12	0.65	3.8 ± 0.1
298	-	-	-0.09	1.81 ± 0.10	0.66	3.3 ± 0.1

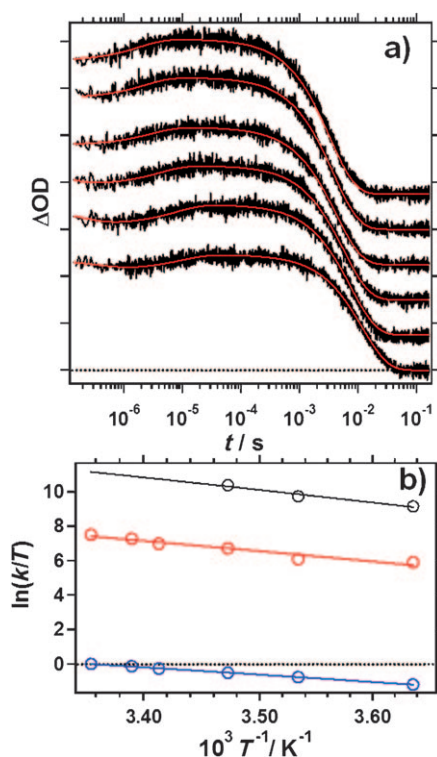


Figure 3. a) Time profiles of the transient absorption signals after photoexcitation at 532 nm of HblCO in a 100 mM phosphate buffer (pH 7) at various temperatures (from top to bottom, $T = 275, 283, 288, 293, 295$ and 298 K). The theoretical fits are shown in red. The temporal profile of the TA signals measured at 298 K can be expressed by a bi-exponential function with relaxation times of $\sim 1.8 \pm 0.1 \mu\text{s}$ and $\sim 3.3 \pm 0.1$ ms. b) The plots show the temperature dependence of three rate constants determined from the fitting of TA signals (τ_1 : black, τ_2 : red and τ_3 : blue).

The temporal profile of the absorbance change in the TA signal can be well expressed by a biexponential function with relaxation times of $\sim 1.8 \pm 0.1 \mu\text{s}$ and 3.3 ± 0.1 ms. The relaxation time of $\sim 1.8 \mu\text{s}$ is consistent with that determined from the TG method ($\sim 1.4 \mu\text{s}$) within an experimental error, indicating that both dynamics share the same origin. The slow dynamics (3.2 ms) is due to the bimolecular recombination of CO

and Hbl. On the other hand, the temperature dependence on the TA signals captured the geminate recombination of the CO ligand that occurs within a rate constant of $9.9 (\pm 8.5) \times 10^6 \text{ s}^{-1}$ ($\sim 101 (\pm 87)$ ns) at 288 K (Table 1). This result indicates that

both dynamics (1.4 μs and 8.7 μs) observed from the TG signals of Hbl are not due to the geminate recombination of the CO ligand. Recently, time-resolved crystallographic experiments^[12] show that the tertiary allosteric transitions occur in a concerted fashion in crystalline Hbl with a rate constant of $6.5 \times 10^4 \text{ s}^{-1}$ (15.4 μs) and precede the subunit rotations that characterize the full R to T transition. These structural transitions observed in the crystalline state appear to correspond to the $\sim 1.4 \mu\text{s}$ dynamics of Hbl in solution determined in the TG and TA measurements. Although the tertiary structural change observed in single crystals is an order of magnitude slower than that in solution phase, this difference is probably due to the tight packing in the Hbl crystals (43.7% solvent). Therefore, considering the previous studies and our experimental results, the $\sim 1.4 \mu\text{s}$ kinetics, which is observed by both the TA and TG techniques, may be attributed to the absorption change of the heme group related with the tertiary structural change rather than the quaternary structural change.

This is against the widely accepted previous assignments of 0.5–2 μs kinetics to R–T quaternary structural transition.^[19,20] Instead we suggest that the dynamics of $\sim 8.7 \mu\text{s}$, which is not observed by the TA technique, should be attributed to the molecular volume change due to the quaternary structural change from R state to T state. This proposed separation of the tertiary structural transitions from the quaternary subunit rotation is supported by time-resolved crystallography studies^[12] in which Knapp et al. observed that the T to R subunit rotation substantially lags formation of the tertiary T-state, with only partial rotation (0.6°) towards the T-state occurring by 80 μs in crystalline Hbl. The difference in the R–T transition dynamics observed in solution and in crystalline state may be due to the molecular contacts in the single crystal that can slow the quaternary transition of Hbl. Furthermore, we could not observe any slower quaternary relaxation following the dynamics of $\sim 8.7 \mu\text{s}$. Thus we suggest the dynamics at $\sim 8.7 \mu\text{s}$ is due to the R–T transition which is the final stage of the conformational dynamic of Hbl. It is worth noting that the two dynamics of $\sim 1.4 \mu\text{s}$ and $\sim 8.7 \mu\text{s}$ (k_{f1} and k_{f2}) have a negative sign of the refractive index change (δn_{f1} and $\delta n_{f2} < 0$) as depicted in Figure 2b. The negative δn_{f1} and δn_{f2} decay over time, indicating

that the absorption change of the heme group due to the tertiary structural change of Hbl (corresponding to δn_{f1}) and the R–T transition (corresponding to δn_{f2}) after photoexcitation of HblCO causes the volume contraction of protein solution in both processes. Also the magnitude of δn_{f1} is larger than that of δn_{f2} by a factor of 3.5, indicating that the volume contraction is larger for the first process ($\sim 1.4 \mu\text{s}$) than the latter ($\sim 8.7 \mu\text{s}$). This volume contraction will be discussed in detail in the next section.

Our comparative results using both TA and TG techniques show that the TA signal is very sensitive to the protein relaxation that takes place in the heme environment of proteins, but can be blind to the overall quaternary structural change. In addition the fact that the $8.7 \mu\text{s}$ kinetics observed in the TG signal but not in the TA signal provides additional evidence that the quaternary structural change does not involve significant change in the heme environment.

Time-resolved photothermal spectroscopic techniques such as the TG and PA methods are useful tools to measure the enthalpy change (ΔH) and the volume (ΔV) change that occur due to optical absorption. In order to elucidate the thermodynamic properties of HblCO, we measured the photoacoustic signals of HblCO and a reference sample (CoCl_2) as a function of temperature using the PA method. Figure 4 shows the representative photoacoustic signal of HblCO and CoCl_2 . The similarity and lack of time shift of the wave-shape for both the sample and reference indicates that only one kinetic process is visible in the experimental time window. From the intercept and slope of the plot of ϕE_{hv} versus $C_p \rho / \beta$, we obtained the values of $\Delta H = 6.8 (\pm 0.1) \text{ kcal mol}^{-1}$ and $\Delta V = 0.12 (\pm 0.07) \text{ mL mol}^{-1}$ for HblCO, indicating that the photodissociation reaction of HblCO is an endothermic reaction and induces a very

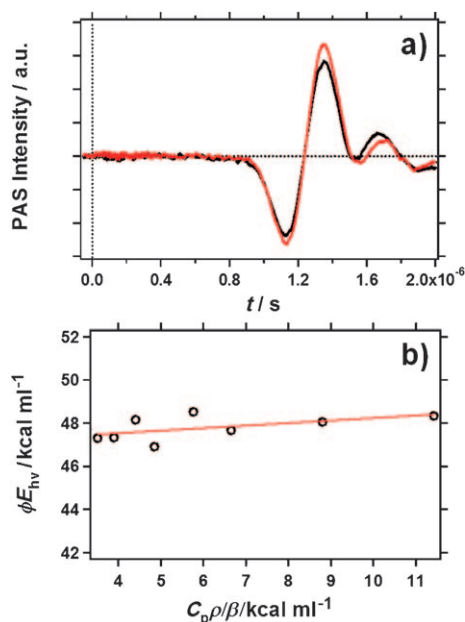


Figure 4. a) PA signals after the photoexcitation of HblCO (black) and the calorimetric reference (red) in a 100 mM phosphate buffer (pH 7). b) Plot of ϕE_{hv} versus $C_p \rho / \beta$ for the photodissociation of CO from Hbl in a 100 mM phosphate buffer (pH 7).

small volume change. Due to the maximum available time delays ($2 \mu\text{s}$) for the PA measurement, the obtained ΔH and ΔV values conveniently correspond to the $\sim 1.4 \mu\text{s}$ process that we attribute to formation of a tertiary T-state.

Here, the reaction enthalpy change for photodissociation of CO from Hbl ($\Delta H = 6.8 \text{ kcal mol}^{-1}$ at pH 7) can be described as $\Delta H = \Delta H_{\text{struct}} + \Delta H_{\text{Fe-CO}}$ where ΔH_{struct} represents the enthalpy change associated with the protein structure relaxation and $\Delta H_{\text{Fe-CO}}$ is the enthalpy change for the Fe–CO bond cleavage and CO solvation upon entering the bulk solvent. Lawsen and Miksovská reported^[22] that the CO-releasing process from a water soluble Fe^{II} meso-tetrakis(4-sulfonatophenyl)-porphyrin ($\text{Fe}^{\text{II}}_4\text{SP}$) having a water molecule ($\text{H}_2\text{O}(\text{Fe}^{\text{II}}_4\text{SP})$) induces the enthalpy change of $20 \pm 4 \text{ kcal mol}^{-1}$. Using a $\Delta H_{\text{Fe-CO}}$ of 20 kcal mol^{-1} , ΔH_{struct} is determined to be $-13 \text{ kcal mol}^{-1}$ at pH 7.

In addition, the reaction volume change (ΔV) can be expressed as $\Delta V = V_{\text{CO}} + V_{\text{Hbl+Water}} - V_{\text{HblCO+Water}}$ where $V_{\text{Hbl+Water}}$ is the partial molar volume of the Hbl solution and $V_{\text{HblCO+Water}}$ is the partial molar volume of the CO-bound Hbl solution. V_{CO} represents the partial molar volume of CO reported previously^[17] to be 35 mL mol^{-1} . From the observed ΔV of 0.12 mL mol^{-1} at pH 7, we estimate that the structural relaxation accompanying the ligand dissociation ($\Delta V_{\text{struct}} = V_{\text{Hbl+Water}} - V_{\text{HblCO+Water}}$) induces a volume decrease of approximately -70 mL mol^{-1} at pH 7. This large volume change associated with the $1.4 \mu\text{s}$ is consistent with the negative δn_{f1} obtained from the TG signals, and is probably due to the entering of solvent water molecules into the dimeric interface as the side-chain of Phe97 (F4) moves from the dimeric interface into a hydrophobic protein cavity. Based on static crystallography measurement Royer and co-workers reported^[10] that after the dissociation of the CO ligand, six water molecules enter into the subunit interface and an additional two water molecules bind to the distal histidine in the heme pocket. Furthermore, they also reported from solution osmotic experiments, about six water molecules bind to the protein upon dissociation of the oxygen ligand, in good agreement with the eight expected based on the crystal structures. These results imply that the large volume contraction due to the structural relaxation of Hbl accompanying ligand dissociation is mainly due to the taking of water molecules into the dimeric protein structure from the outer solvent. As we noted, the δn_{f2} has a smaller magnitude than δn_{f1} as a factor of 3.5, indicating that the process associated with δn_{f2} , the $8.7 \mu\text{s}$ that we attribute to the R–T transition, involves relatively smaller volume contraction. We suggest that formation of the tertiary T-state involves addition of most of the new water molecules, perhaps six, but that the quaternary subunit rotation may be required for binding the final T-state water molecules. Inspection of a model for the tertiary T-state reveals close contacts for interface T-state water molecules binding near the heme propionates that could prevent binding of the last two water molecules until the quaternary transition occurs. Assembly of the complete interface T-state water cluster may provide some of the driving force for the quaternary transition.

We also measured the potential energy barrier for the conformational dynamics of Hbl followed by the dissociation of CO ligand using the TA method. To determine the energy barrier for the conformational dynamics of Hbl, TA experiments were carried out at various temperatures as shown in Figure 3b. The temporal profile of the absorbance change in the TA signal in the low temperatures can be well expressed by a tri-exponential function, while the temporal profile of the absorbance change in the TA signal at the higher temperature range can be well expressed by a bi-exponential function. The analyzed decay times for TA signals are summarized in Table 1. As explained previously, τ_1 , τ_2 and τ_3 are due to the geminate recombination of the dissociated CO ligand, the absorption change of the heme group in Hbl followed by the photodissociation of the CO ligand and the bimolecular recombination of CO and Hbl, respectively. Using the Eyring equation, $\ln(k/T) = -(\Delta H^\ddagger/RT) + \ln(k_B/h) + (\Delta S^\ddagger/R)$, the activation enthalpy (ΔH^\ddagger) and the activation entropy (ΔS^\ddagger) for the absorption change of the heme group in Hbl are determined to be $11.9 \pm 1.5 \text{ kcal mol}^{-1}$ and $7.5 \pm 0.7 \text{ cal mol}^{-1} \text{ K}^{-1}$, respectively. Furthermore, the energy barriers for the geminate recombination of CO ligand are $\Delta H^\ddagger = 14.4 \pm 2.7 \text{ kcal mol}^{-1}$ and $\Delta S^\ddagger = 23.5 \pm 3.2 \text{ cal mol}^{-1} \text{ K}^{-1}$.

In conclusion, we have studied the conformational dynamics and thermodynamics of Hbl, which is an excellent model system for studying the allosteric regulation and cooperative ligand binding with combined probes of TG, TA and PA techniques. Our study combining TG, TA and PA methods and previous studies allow us to propose comprehensive reaction pathways for the R–T transition of Hbl as shown in Figure 5. Upon CO photodissociation of HbICO, some of Hbl survive from the fast geminate CO recombination and form a tertiary T-state with the time constant of $\sim 1.4 \mu\text{s}$. In this process the heme relaxation occurs and water molecules enter the subunit interface. This intermediate undergoes further subunit rotation to form the T-state Hbl with the timescale of $8.7 \mu\text{s}$. The quaternary subunit rotation may be required for binding the final T-state water molecules. Both processes are captured in the TG signals but only the $1.4 \mu\text{s}$ is visible in the TA signal. Our comparative results using both TA and TG techniques show that the TA signal is sensitive to the protein relaxation that takes place in the heme environment of proteins, but can be blind to the overall quaternary structural change.

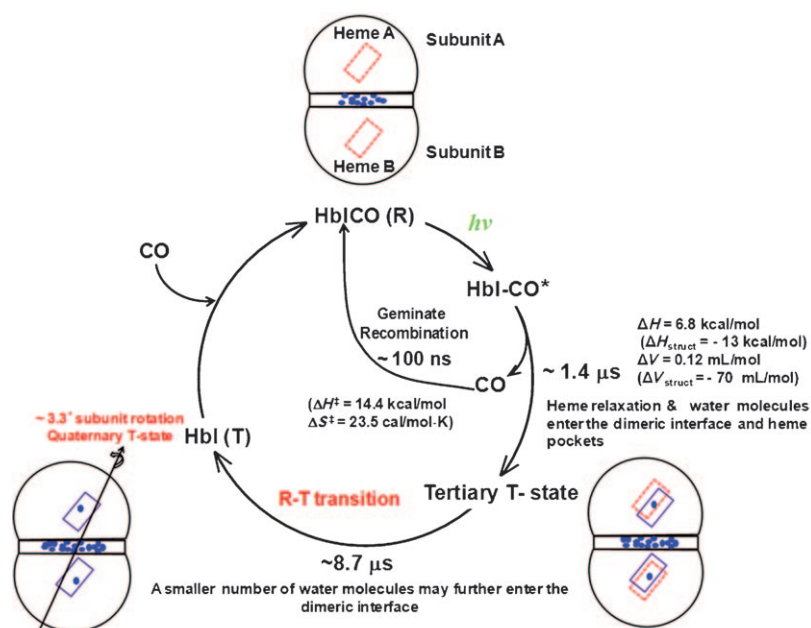


Figure 5. Schematic illustration of the conformational dynamics and kinetics scheme of the HbICO photodissociation photocycle in the solution phase determined by combined probes of TG, TA and PA spectroscopy. Immediately after photodissociation the tertiary T state is formed through heme relaxation ($\sim 1.4 \mu\text{s}$) and water molecules (blue circles) enter the dimeric interface and heme pockets. The tertiary T state and R state heme positions are indicated in solid line rectangle (violet color) and dashed line rectangle (red color) respectively. The complete Hbl (T) state is achieved through 3.3° quaternary subunit rotation and a smaller number of water molecules may further enter the dimeric interface with a rate constant of $1.2 \pm 0.6 \times 10^5 \text{ s}^{-1}$.

Experimental Section

The Hbl was over-expressed in *Escherichia coli* and purified as described previously.^[23] HbICO was prepared by the following method. A Hbl solution in 100 mM phosphate buffer (pH 7) was put into a rubber-topped air-tight quartz cuvette (optical path length = 2 mm) and the concentrations of Hbl were adjusted to be 0.5 mM. The Hbl is reduced by adding 10 μL of 1 M sodium dithionite solution to the Hbl solutions under a nitrogen atmosphere. CO gas was passed over the reduced samples for 30 min to convert Hbl to the CO-bound Hbl (HbICO). The sample solutions were prepared just before measurement.

The experimental setups for the TG, TA and photoacoustic experiments are similar to those reported previously.^[24–32] More details are provided in the Supporting Information.

Acknowledgements

This work was supported by Creative Research Initiatives (Center for Time-Resolved Diffraction) of MEST/NRF.

Keywords: homodimeric hemoglobin • protein structures • structure-activity relationships • time-resolved spectroscopy • transient grating

- [1] F. J. Roughton, *J. Gen. Physiol.* **1965**, *49*, Suppl:105–126.
- [2] E. Chiancone, P. Vecchini, D. Verzili, F. Ascoli, E. Antonini, *J. Mol. Biol.* **1994**, *235*, 657–681.
- [3] W. E. Royer Jr., *J. Mol. Biol.* **1994**, *235*, 657–681.
- [4] M. F. Perutz, *Nature* **1970**, *228*, 726–739.

- [5] J. Baldwin, C. Chothia, *J. Mol. Biol.* **1979**, *129*, 175–220.
- [6] B. Shaanan, *J. Mol. Biol.* **1983**, *171*, 31–59.
- [7] G. Fermi, M. F. Perutz, B. Shaanan, R. Fourme, *J. Mol. Biol.* **1984**, *175*, 159–174.
- [8] J. E. Knapp, Q. H. Gibson, L. Cushing, W. E. Royer, Jr., *Biochemistry* **2001**, *40*, 14795–14805.
- [9] J. E. Knapp, W. E. Royer, Jr., *Biochemistry* **2003**, *42*, 4640–4647.
- [10] W. E. Royer, Jr., A. Pardani, Q. H. Gibson, E. S. Peterson, J. M. Friedman, *Proc. Natl. Acad. Sci. USA* **1996**, *93*, 14526–14531.
- [11] J. E. Knapp, M. A. Bonham, Q. H. Gibson, J. C. Nichols, W. E. Royer, Jr., *Biochemistry* **2005**, *44*, 14419–14430.
- [12] J. E. Knapp, R. Pahl, V. Srajer, W. E. Royer, Jr., *Proc. Natl. Acad. Sci. USA* **2006**, *103*, 7649–7654.
- [13] Y. Nakasone, T. A. Ono, A. Ishii, S. Masuda, M. Terazima, *J. Am. Chem. Soc.* **2007**, *129*, 7028–7035.
- [14] K. Tanaka, Y. Nakasone, K. Okajima, M. Ikeuchi, S. Tokutomi, M. Terazima, *J. Mol. Biol.* **2009**, *386*, 1290–1300.
- [15] M. Sakakura, S. Yamaguchi, N. Hirota, M. Terazima, *J. Am. Chem. Soc.* **2001**, *123*, 4286–4294.
- [16] M. Terazima, *Phys. Chem. Chem. Phys.* **2005**, *8*, 545–557.
- [17] T. Hara, N. Hirota, M. Terazima, *J. Phys. Chem.* **1996**, *100*, 10194–10200.
- [18] M. E. Young, P. A. Carroad, R. L. Bell, *Biotechnol. Bioeng.* **1980**, *22*, 947–955.
- [19] E. Chiancone, R. Elber, W. E. Royer, Jr., R. Regan, Q. H. Gibson, *J. Biol. Chem.* **1993**, *268*, 5711–5718.
- [20] J. C. Nichols, W. E. Royer, Jr., Q. H. Gibson, *Biochemistry* **2006**, *45*, 15748–15755.
- [21] D. L. Rousseau, S. Song, J. M. Friedman, A. Boffi, E. Chiancone, *J. Biol. Chem.* **1993**, *268*, 5719–5723.
- [22] J. Miksovská, J. Norstrom, R. W. Larsen, *Inorg. Chem.* **2005**, *44*, 1006–1014.
- [23] C. M. Summerford, A. Pardani, A. H. Betts, A. R. Poteete, G. Colotti, W. E. Royer, Jr., *Protein. Eng.* **1995**, *8*, 593–599.
- [24] T. Nada, M. Terazima, *Biophys. J.* **2003**, *85*, 1876–1881.
- [25] N. Baden, M. Terazima, *J. Phys. Chem. A* **2006**, *110*, 15548–15555.
- [26] J. Choi, Y. O. Jung, J. H. Lee, C. Yang, B. Kim, H. Ihee, *ChemPhysChem* **2008**, *9*, 2708–2714.
- [27] J. Choi, M. Terazima, *Photochem. Photobiol. Sci.* **2003**, *2*, 767–773.
- [28] L. B. Luo, G. Li, H. L. Chen, S. W. Fu, S. Y. Zhang, *J. Chem. Soc. Dalton Trans.* **1998**, 2103–2107.
- [29] G. Li, F. F. Zhang, H. Chen, H. F. Yin, H. L. Chen, S. Y. Zhang, *J. Chem. Soc. Dalton Trans.* **2002**, 105–110.
- [30] H. Chen, G. Li, F. F. Zhang, L. Sun, H. L. Chen, S. Y. Zhang, *Spectrochim. Acta. A. Mol. Biomol. Spectrosc.* **2003**, *59*, 2767–2774.
- [31] K. S. Peters, T. Watson, T. Logan, *J. Am. Chem. Soc.* **1992**, *114*, 4276–4278.
- [32] H. Chen, L. Sun, G. Li, S. Y. Zhang, H. L. Chen, *Biochem. Biophys. Res. Commun.* **2004**, *319*, 157–162.

Received: October 21, 2009

Published online on November 18, 2009